Modeling Parison Formation in Extrusion Blow Molding by Neural Networks

Han-Xiong Huang, Song Lu

Center for Polymer Processing Equipment and Intellectualization, College of Industrial Equipment and Control Engineering, South China University of Technology, Guangzhou, People's Republic of China

Received 1 March 2004; accepted 15 September 2004
DOI 10.1002/app.21700
Published online in Wiley InterScience (www.interscience.wiley.com).

ABSTRACT: A series of experiments were carried out on the parison formation stage in extrusion blow molding of high-density polyethylene (HDPE) under different die temperature, extrusion flow rate, and parison length. The drop time of parison when it reached a given length and its swells, including the diameter, thickness, and area swells, were determined by analyzing its video images. Two back-propagation (BP) artificial neural network models, one for predicting the length evolution of parison with its drop time, the other predicting the swells along the parison, were constructed based on the experimental data. Some modifications to the original BP algorithm were carried out to speed it up. The comparison of the predicted parison swells using the trained BP network models with the experimentally determined ones showed quite a good agreement between the two. The sum of squared error for the predictions is within 0.001. The prediction of the parison diameter and thickness distributions can be made online at any parison length or any parison drop time within a given range using the trained models. The predicted parison swells were analyzed. © 2005 Wiley Periodicals, Inc. J Appl Polym Sci 96: 2230–2239, 2005

Key words: extrusion; modeling; molding; plastics

INTRODUCTION

Blow molding represents the third largest plastics processing technique worldwide for manufacturing many different products in the plastics industry, accounting for 10 wt % of all plastics. It is also one of the fastest growing industries worldwide.[1] Extrusion blow molding is a major blow molding category, with a product range from packaging containers to industrial complex parts such as those supplied to the automobile, office automation equipment, and pharmaceutical sectors, etc. It has a number of technical and economical advantages concerning the low-pressure characteristic of the process and the facility to produce complex-shaped parts with very thin walls.

The extrusion blow molding process consists of three main stages, namely, parison formation, parison inflation, and part cooling and solidification. Parison formation is a critical stage. It is also rather complex in that the parison dimensions, including the diameter and thickness, are affected by two phenomena known as swell and sag. The parison swell, occurring both in diameter and thickness, is due to the nonlinear viscoelastic deformation imposed on the polymer melt during its flow in the extrusion die. The degree of swell is dependent on materials characteristics and processing parameters. In general, anything that increases the elastic response of the melt will lead to greater swell. The geometry of the flow channel within the die has a strong effect on the swell. Sag, or drawdown, results from the tensile stress generated by gravity acting on the parison while it hangs from the die. A polymer with a lower molecular weight exhibits a great degree of sag. Increasing the melt temperature, suspension time, and/or total parison length also results in a great degree of sag.

The parison dimensions just prior to inflation are critical to the inflation stage, since these dimensions constitute the starting point of the inflation stage and directly influence the final part dimension distribution.[2] Blow molded parts must meet strict dimension distribution requirements to provide the necessary strength and rigidity with minimum material usage. So it is critical to be able to predict the parison dimensions.

There is considerable effort in modeling the parison formation stage to predict the parison dimensions. Two approaches can be identified: semiempirical approaches[3–5] and numerical simulation methods. By using numerical methods, the polymer melt is consid-

Correspondence to: H.-X. Huang (mmhuang@scut.edu.cn).
Contract grant sponsor: The National Natural Science Foundation of China; contract grant number: 50390096.
Contract grant sponsor: SRFDP; contract grant number: 20010514002.
Contract grant sponsor: Teaching and Research Award Program for Outstanding Young Teachers in Higher Education Institutions of MOE, People's Republic of China.

ered as a Newtonian fluid[6–8] or a non-Newtonian fluid. For the latter, two types of constitutive models, differential[9–12] and integral equations,[2,13–17] are used.

Numerical simulations on the parison formation help minimize machine setup times and tooling costs, as well as optimizing processing parameters to yield desired final part specifications. However, the following shortcomings should be taken into account:

1. Simulations generally require many simplifying assumptions, thereby resulting in a limited accuracy of simulation results.
2. A constitutive equation must be used. Clearly, reliable constitutive equations for adequately describing the nonlinear viscoelastic behavior of the polymer melt during extrusion are still lacking. Otsuki et al.[15] carried out numerical simulations of parison swells extruded through straight, divergent, and convergent dies. Several important viscoelastic models, the K-BKZ, the PTT, and the Larson models, which can express well the shear flow characteristics of high-density polyethylene (HDPE), were used. Their studies demonstrated that there are remarkable differences among the results of these viscoelastic models. Furthermore, there are some difficulties in obtaining relevant rheological data for constitutive equations.
3. There are some limitations and complications. Numerical simulations have no ability to handle effects of parison programming (time dependent gap variation), coupled effects of sag, and the prediction of swell at higher shear rate levels of industrial blow molding machines.[16] In addition, because of the complexity of the equations involved, these simulations are quite time consuming.

Artificial neural networks (ANNs) are mathematical models developed to mimic certain information storing and processing capabilities of the brain of higher animals. ANNs have been applied widely to various areas. The advantages of employing ANNs over simulations based on numerical techniques include:

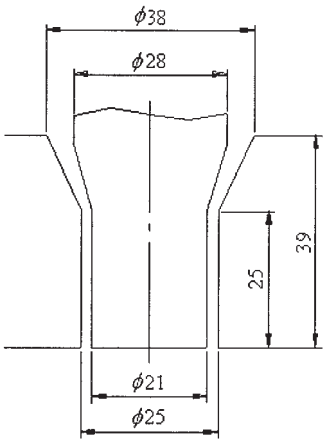

Figure 1 Parison die used in the experiments. All dimensions are in mm.

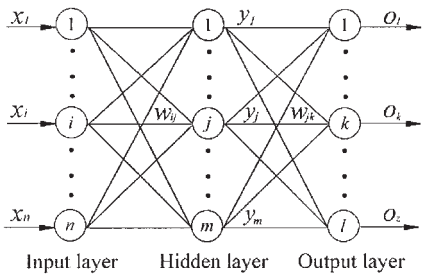

Figure 2 Typical BP neural network with three layers.

1. No or a minimal number of simplifying assumptions.
2. No need for constitutive equations, and thus no need for difficult-to-obtain rheological data.
3. Online prediction for process monitoring and control.
4. Faster response.

DiRaddo and Garcia-Rejon[18,19] utilized the neural network method to predict final part dimensions from initial parison dimensions and initial parison dimensions from the specified final part thickness, respectively. Huang and Liao[20,21] utilized the neural network method to predict swells of the parison under the effect of sag in the extrusion blow molding of HDPE and HDPE/polyamide-6 (PA-6) blends. It was demonstrated that the neural network model can predict the parison swells with a high degree of precision. The prediction, however, could be made only on the parison with a specified length because the parison length was set at a fixed value. The target in this work is to predict the dimension distributions of the parison at any length or any drop time during its formation process using the neural network method.

A back-propagation (BP) neural network, selected in this work, is successfully used in many fields. However, it has been realized that the original BP algorithm is too slow for most practical applications, and many modifications have been suggested to speed it up.[22–24] So another aim of this work is to carry out some modifications to the original BP algorithm to speed it up.

EXPERIMENTAL

The material used is an HDPE 5300B manufactured by Petrochina Daqing Petrochemical Co. This HDPE is an extrusion blow molding grade resin with a melt index of 0.41 g/10 min and a solid density of 0.952 g/cm^3.

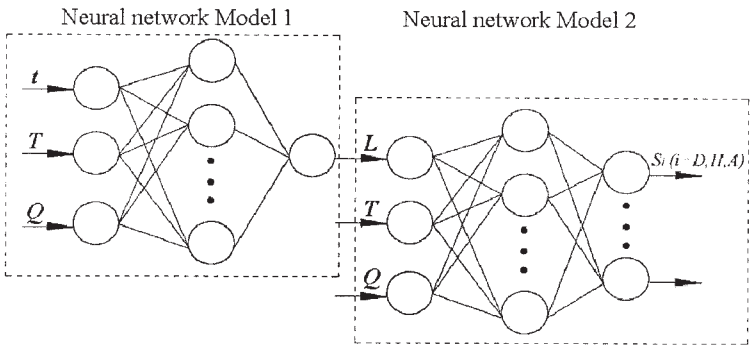

Figure 3 Schematic of BP neural network architecture used in this work.

An extrusion blow molding machine with a screw diameter of 45 mm and a length-diameter-ratio of 25 : 1 was used. The annular die used to extrude the parison was a straight one, shown in Figure 1, with an outer diameter of 25 mm and a lip gap of 2 mm. A video capture system was employed to access the images of the parison online. The capture system mainly includes a color video camera and a video capture card. The former is mounted perpendicular to the axis of the parison, and the latter is installed in a personal computer. The analog signal from the former is sent to the latter, which digitizes and compresses the video images in one step, directly onto the hard disk of the computer.

During the extrusion of the parison, ink marks were put on its outer surface just below the die exit at the same time interval. To predict the dimensions of the parison during its formation using the neural network method, images with five different parison lengths, 100, 150, 200, 250, and 300 mm, respectively, were captured. Twenty marks were put on the parison with different lengths.

By analyzing the digitized video images of the parison, the outer diameter (D_p) corresponding to each ink mark and the distance (Δl) between two adjacent ink marks could be determined. Next, the thickness (H_p) for each parison segment, assuming cylindrical symmetry, could be calculated on the basis of mass conservation[25]:

$$H_p = \frac{D_p}{2} - \sqrt{\left(\frac{D_p}{2}\right)^2 - \frac{Q\Delta t}{\pi\rho\Delta l}} \tag{1}$$

where Q is the extrusion flow rate, (Δt) the time between two adjacent ink marks, and ρ the melt density of the material used. Then the diameter, thickness, and area swells, denoted by S_D, S_H, and S_A, respectively, could be calculated. Among them, S_A was calculated by:

$$S_A = S_D S_H \tag{2}$$

The corresponding time when the parison reached each length could be determined by analyzing the images. For each parison length, three different die temperatures, 170, 200, and 230°C, and four different extrusion flow rates, 4.8, 10.3, 15.2, and 17.1 kg/h, were employed. Thus, 60 ($5 \times 3 \times 4$) sets of data, that is, 60 sets of the drop time of the parison and its diameter, thickness, and area swell values, with different length extruded at different processing parameters, were obtained.

TABLE I
Drop Time of the Parison with Different Lengths under Various Processing Conditions

Parison length (mm)	Parison drop time (s)											
	4.8[a]			10.3			15.2			17.1		
	170[b]	200	230	170	200	230	170	200	230	170	200	230
100	13.5	13.0	12.6	6.8	6.4	6.1	4.8	4.6	4.4	4.2	4.0	3.9
150	22.7	21.1	19.5	11.9	11.0	10.2	8.6	8.1	7.7	7.7	7.2	6.8
200	29.7	27.3	25.2	15.5	14.2	13.1	11.3	10.6	10.1	10.0	9.4	9.0
250	36.5	32.9	31.2	18.7	17.3	16.0	13.8	13.1	12.3	12.7	11.6	11.2
300	41.9	39.1	36.7	21.8	20.0	18.8	16.4	15.5	14.4	14.9	13.8	13.3

[a] Flow rate (kg/h);
[b] Die temperature (°C).

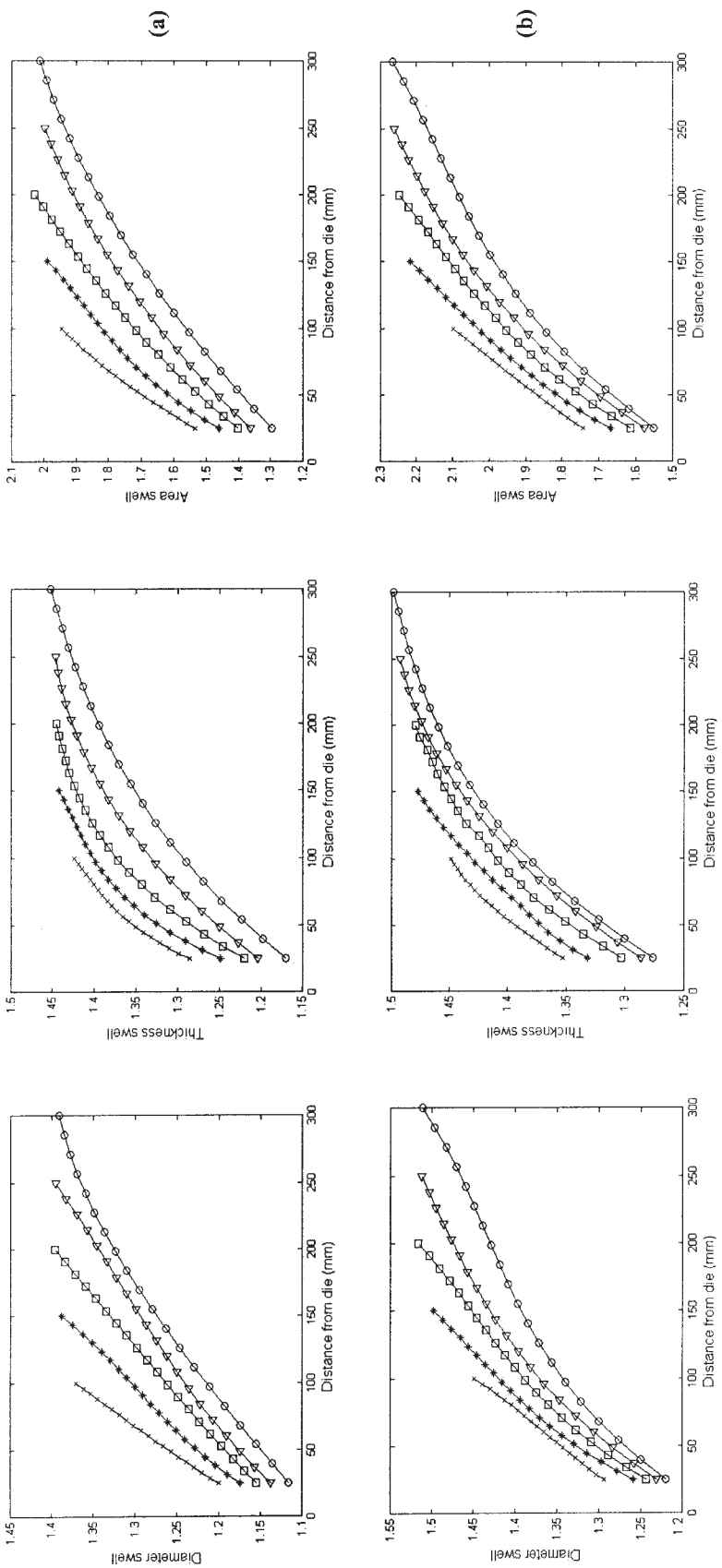

Figure 4 Experimentally determined diameter, thickness, and area swells of the parison with a length (mm) of (×) 100, (*) 150, (□) 200, (△) 250, and (○) 300. (a) $T = 230°C$, $Q = 4.8$ kg/h; (b) $T = 170°C$, $Q = 17.1$ kg/h.

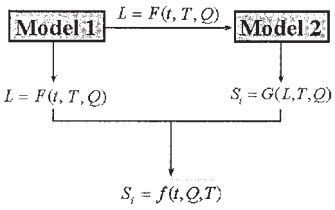

Figure 5 Relationship between network Models 1 and 2.

NEURAL NETWORK DESIGNING AND TRAINING

Determination of the network architecture

The BP network, used in this study, has hierarchical feed forward network architecture constituted by a highly interconnected set of processing units, called neurons, which are arranged in a layered structure. It has been shown that one hidden layer BP network with "sufficient" processing elements can approximate any function to an arbitrary precision. So a BP network (shown in Fig. 2) with three layers, namely, input layer, hidden layer, and output layer, was used in this work. The input layer receives and distributes the input pattern, the hidden layer captures the nonlinearities of the input–output relationship, and the output layer produces the output pattern. An input vector, $\boldsymbol{X} = (x_1, x_2, \ldots, x_i, \ldots, x_n)^{\mathrm{T}}$, is applied to the input layer of the network. The output of the ith neuron in the input layer is its input x_i. Then for the hidden layer:

$$net_j = \sum_{i=1}^{n} w_{ij}\, x_i + \theta_j \tag{3}$$

$$y_j = f(net_j) \tag{4}$$

where net_j is the net input to the jth neuron in the hidden layer and y_j is its output, w_{ij} is the connection weight from the ith input unit to the jth neuron in the hidden layer, and θ_j is the threshold value of the jth neuron.

For the output layer:

$$net_k = \sum_{j=1}^{m} w_{jk}\, y_k + \theta_k \tag{5}$$

$$o_k = f(net_k) \tag{6}$$

where net_k is the net input to the kth neuron in the output layer and o_k is its output, w_{jk} is the connection weight from the jth input unit to the kth neuron in the output layer, and θ_k is the threshold value of the kth neuron.

The function $f(x)$ in eqs. (4) and (6) is the transfer function. Here the sigmoid transfer function was used:

$$f(x) = \frac{1}{1 + e^{-x}} \tag{7}$$

Two BP network models with three layers, shown in Figure 3, were constructed in this work. The number of neurons in the input layer and the output layer was determined according to the parameters involved in the problem investigated. For network Model 1, the number of neurons in the input layer and the output layer is 3 and 1, respectively. The 3 input parameters are the parison drop time (t) from the start of extrusion, die temperature (T), and extrusion flow rate (Q), respectively. The 1 output parameter is the parison length (L) corresponding to the time of t. For Model 2, the number of neurons in the input layer and the output layer is 3 and 20, respectively. The 3 input parameters are L, T, and Q, respectively. The 20 output parameters are the predicted diameter, thickness, or area swells of 20 points along the parison during its formation process.

There is not yet theoretical guidance to the determination of the number of neurons in the hidden layer. Here it was determined through experimentation. Four and 16 hidden neurons were finally selected for network Models 1 and 2, respectively.

TABLE II
Sum of Squared Error (SSE) for the Parison Swells Predicted from Network Model 2

Network inputs			SSE ($\times 10^{-3}$)		
Die temperature (°C)	Flow rate (kg/h)	Parison length (mm)	Diameter swell	Thickness swell	Area swell
170	10.3	200	0.82053	0.90173	0.92354
170	17.1	300	0.50024	0.66183	0.77301
200	4.8	100	0.31926	0.42738	0.43398
200	15.2	250	0.48325	0.75859	0.77239
230	4.8	300	0.93171	0.98248	0.99854
230	15.2	150	0.48663	0.58862	0.74293

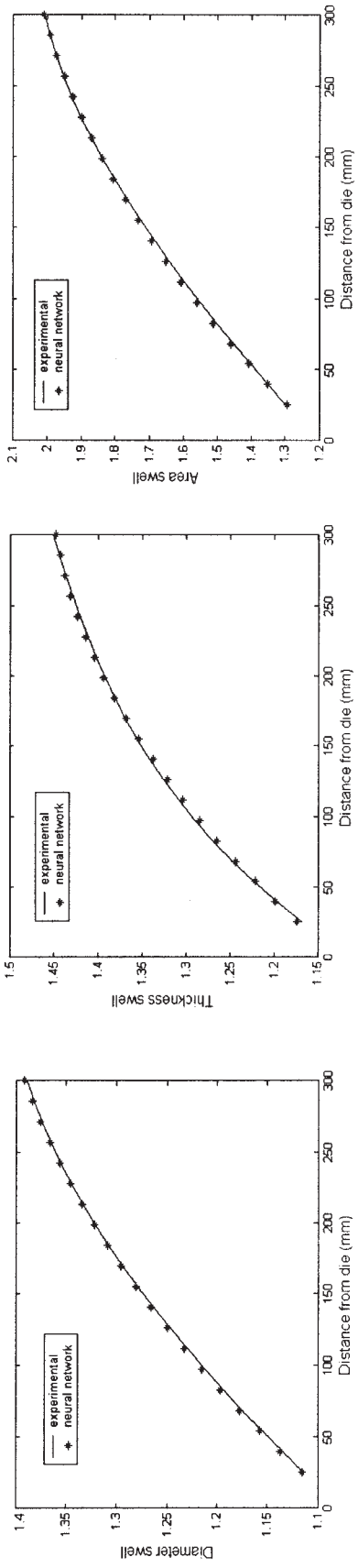

Figure 6 Comparison of predicted diameter, thickness, and area swells of parison from network Model 2 with experimental results. $T = 230°C$, $Q = 4.8$ kg/h.

Network training and testing

As mentioned in the Experimental section, 60 data sets were obtained from experiments by changing the die temperature, extrusion flow rate, and parison length (i.e., parison drop time) for each network model. For Model 1, 55 among the 60 data sets were used as training patterns to train the neural network to ascertain its weight and threshold values. The remaining 5 data sets were used as testing patterns to test the trained neural network to verify the model. For Model 2, 54 data sets were used as training patterns, and the remaining 6 data sets were used as testing patterns.

It is usually necessary to preprocess the data before presenting the patterns to the BP network, because the sigmoid transfer function [see eq. (7)] modulates the output of each neuron to values between 0 and 1. Here the following normalization procedure was used:

$$V' = \frac{V - V_{\min}}{V_{\max} - V_{\min}} \times 0.8 + 0.1 \tag{8}$$

where V is the original data, $V_{\min}$ and $V_{\max}$ the minimum and maximum values of V, respectively, and V' the normalized data of the corresponding V. Thus, each value V is scaled to its normalized value, V', between 0.1 and 0.9.

Initial weight and threshold values were chosen randomly between 0 and 1. A modified BP learning algorithm, with a momentum term and a self-adaptive learning rate coefficient was utilized. The momentum coefficient was set at 0.8, and the initial learning rate coefficient was set at 0.01; the values of 1.1 and 0.7 for the learning rate coefficient increasing factor and for the learning rate coefficient decreasing factor, respectively, were used. The learning rate coefficient was continuously modified during training.

The networks were trained by repeatedly accessing the entire set of training patterns that incorporated the coupled effects of the die temperature, flow rate, and parison drop time (i.e., parison length). The network gradually "learned" the input–output relationship of interest by adjusting the weights to minimize the error between the actual and predicted output patterns of the training set. Once the sum of squared error for the training patterns reduced within a given tolerance (set at 0.001 in this study), or the number of training iterations reached a predetermined one (set at 50,000 in this study), the network training course was stopped.

Finally, the trained networks were tested through several sets of input data, different from those used in the training stage, to examine the validity of the models in predicting the outputs.

RESULTS AND DISCUSSION

During the formation of the parison, its profiles were captured continuously using the visualization tech-

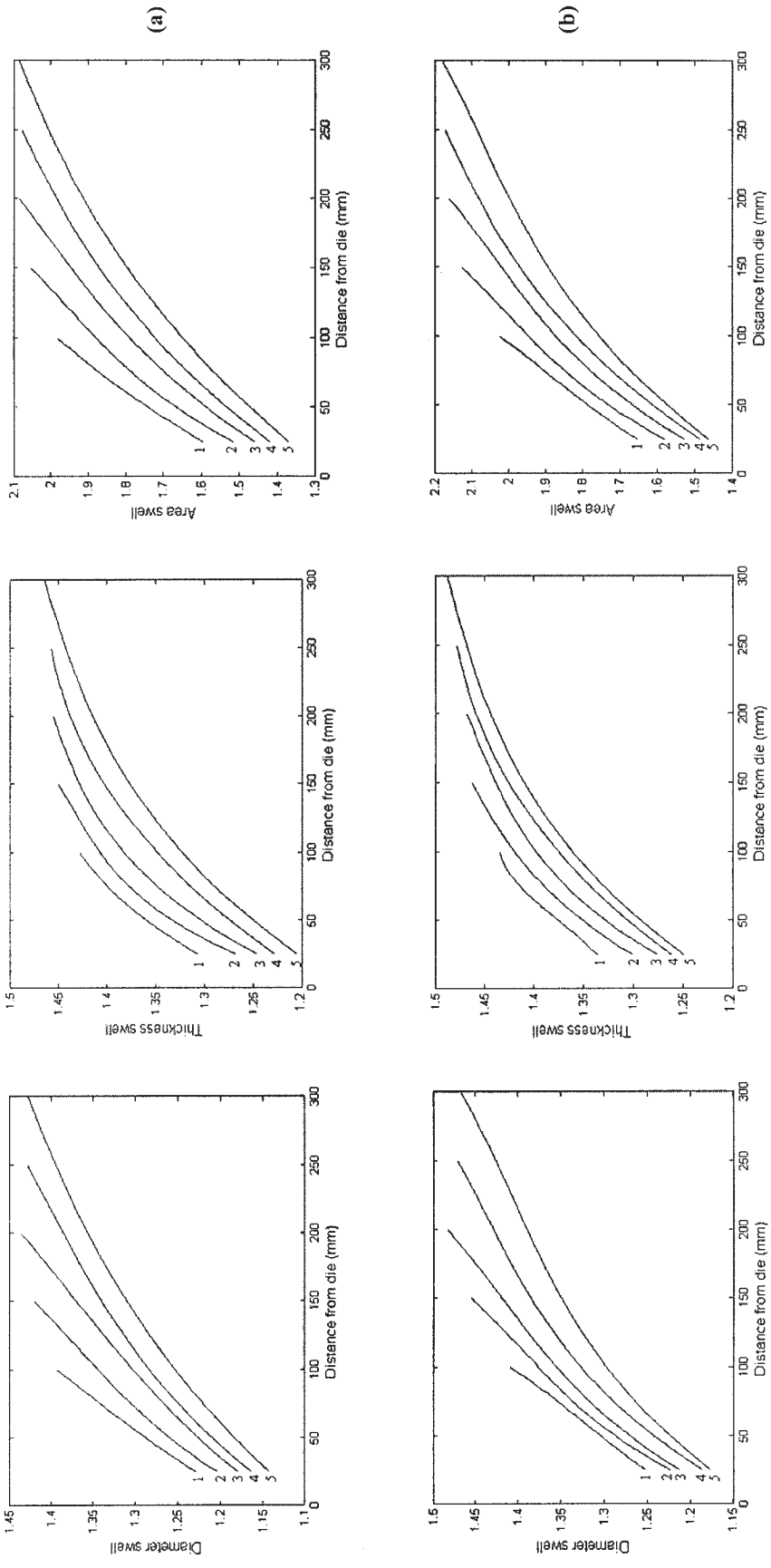

Figure 7 Predicted parison diameter, thickness, and area swells for different lengths (mm): (1) 100; (2) 150; (3) 200; (4) 250; (5) 300. (a) $T = 210°C$, $Q = 10$ kg/h; (b) $T = 200°C$, $Q = 16$ kg/h.

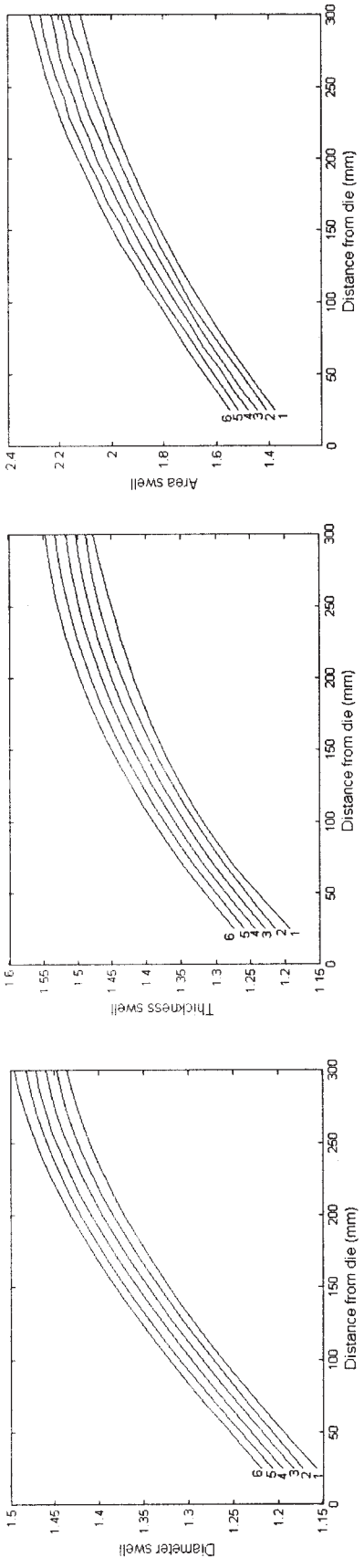

Figure 8 Predicted parison diameter, thickness, and area swells at six different flow rates (kg/h): (1) 5; (2) 7.5; (3) 10.0; (4) 12.5; (5) 15.0; (6) 17.0. T = 190°C.

nique. By analyzing the video images of the parison extruding at different processing parameters and parison lengths, the drop time when it reached a given length and its diameter swell were determined. Then the parison thickness and area swells were calculated on the basis of the diameter swell. Table I shows the drop time of the parison with different lengths under various processing conditions. Some results of the parison swells, including the diameter, thickness, and area swells, are shown in Figure 4.

As mentioned above, the neural networks were trained by accessing a pool of training data sets. As shown in Figure 5, after being trained, Model 1 ascertains the quantitative relationship between the parison length and the parison drop time, die temperature, and flow rate, that is, $L = F(t,T,Q)$; and Model 2 ascertains the quantitative relationship between the parison swells and the parison length, die temperature, and flow rate, that is, $S_i = G(L,T,Q),(i = D,H,A)$. Then, combining both models, the quantitative relationship between the parison swells and the parison drop time, die temperature, and flow rate, that is, $S_i = f(t,Q,T),(i = D,H,A)$, was established. This means that the swells can be predicted at any time within a given range during the parison formation process.

After testing the trained network, the error between the predicted output value from the network model and the experimental value could be obtained. The trained neural network Model 1 shows a high degree of prediction precision (the relative error between predicted parison length from Model 1 and the experimentally determined one is less than 0.01). Table II gives the sum of the squared error (SSE) for the parison swells predicted from Model 2. As can be seen, the SSE for the thickness swell is slightly larger than that for the diameter swell. The area swell has the largest SSE among the three kinds of swells. This may be attributed to the fact that the thickness swell was calculated indirectly from the measured diameter swell, and the area swell was calculated indirectly from the measured diameter swell and the calculated thickness swell. However, no matter for the diameter swell, the thickness swell, or the area swell, the SSE is very small (less than 0.001), that is, the trained neural network model shows a high degree of prediction precision. The comparison between the predicted parison swells from the trained network Model 2 and the corresponding experimental results is also shown in Figure 6. It can be clearly observed that quite a good agreement is obtained between the two.

Once trained and tested, the neural network models have been identified and can be used to predict the outputs expected for new levels of input variables. Thus, the parison lengths and swells, including diameter, thickness, and area swells, under the effect of sag, can be predicted from processing parameters resorting

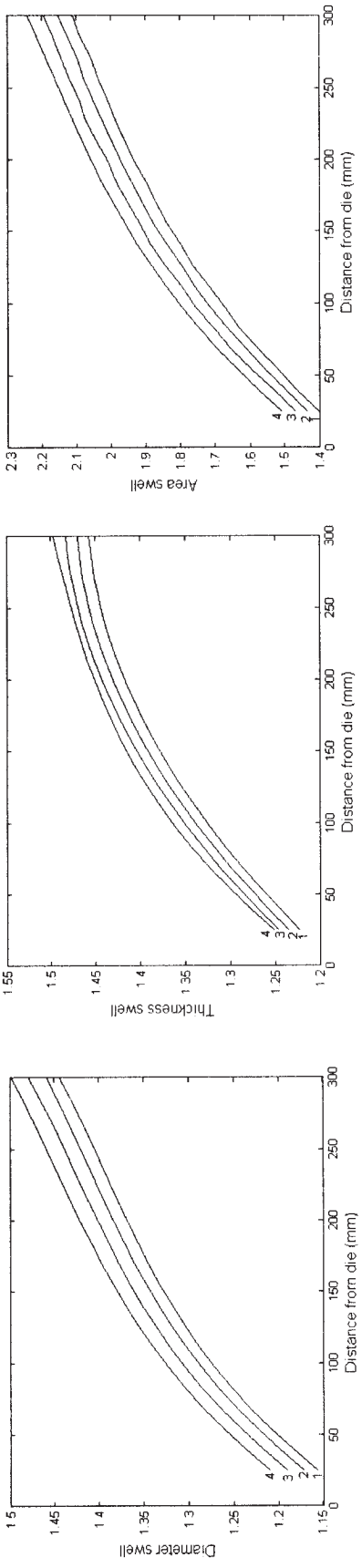

Figure 9 Predicted parison diameter, thickness, and area swells at four different die temperatures (°C): (1) 230; (2) 210; (3) 190; (4) 170. Q = 13kg/h.

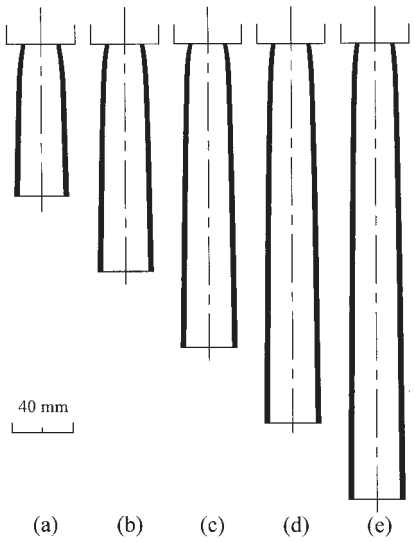

Figure 10 Predicted parison profiles at different time(s): (a) 4.5; (b) 7.5; (c) 10.0; (d) 12.5; (e) 14.5. T = 210°C, Q = 16.5 kg/h.

to the network models, thereby reducing the amount of experimental work.

Some results of the swell prediction of the parison with different lengths by the network models are shown in Figure 7. As can be seen, the swells at the same distance from the die exit decrease gradually with increasing the parison length. This is caused by weight that acts on the suspended parison. Moreover, the swells at the extreme bottom of the parison first increase with the parison length. After the parison length exceeds a certain value (about 100 ~ 150 mm), the swells at the bottom tend to plateau values, that is, the ultimate swells. This is because no weight acts on the parison bottom and so the swells at the bottom are mainly affected by the viscoelastic recovery, which has completed after the parison reaches a long enough length.

Figures 8 and 9 illustrate the parison diameter, thickness, and area swells predicted by the network models at six different flow rates and four different die temperatures, respectively. As expected, swells increase as the flow rate increases or the melt temperature decreases.

The above predictions were carried out using network Model 2. As mentioned above, combining neural Models 1 and 2, the parison swells can be predicted at any time during the parison formation. Figure 10 shows the parison profiles predicted from combining the two models at different times. As can be seen, there is a sharp increase for the diameter and thickness of the parison near the die exit. Then the dimensions tend to decrease with time under the action of sag.

The predictions mentioned above can be made online for the purposes of process monitoring and control.

CONCLUSIONS

Two back-propagation (BP) neural network models have been constructed based on experimental data for the parison formation in extrusion blow molding of high-density polyethylene (HDPE). The length evolution of the parison with its drop time can be predicted at different processing conditions using Model 1. The parison swells, including the diameter, thickness, and area swells, can be predicted from Model 2 for different parison length. Combining these two BP network models, the swells can be predicted at any time within a given range during the parison formation process with a high degree of precision.

This work also carried out some modifications to the original BP algorithm to speed it up.

References

1. Rosato, D. V.; Rosato, A. V.; DiMattia D. P., Eds.; Blow Molding Handbook; Hanser: Munich, 2004; 2nd ed.
2. Garcia-Rejon, A.; DiRaddo, R. W.; Ryan, M. E. J Non-Newtonian Fluid Mech 1995, 60, 107.
3. Ajroldi, G. Polym Eng Sci 1978, 18, 743.
4. Basu, S.; Fernandez, F. Adv Polym Technol 1983, 3, 143.
5. DiRaddo, R. W.; Garcia-Rejon, A. Polym Eng Sci 1992, 32, 1401.
6. Mitsoulis, E. AIChE J 1986, 32, 497.
7. Seo, Y.; Wissler, E. H. J Appl Polym Sci 1989, 37, 1159.
8. Seo, Y. J Appl Polym Sci 1990, 41, 25.
9. Tanoue, S.; Kuwano, Y.; Kajiwara, T.; Funatsu, K. Polym Eng Sci 1995, 35, 1546.
10. Tanoue, S.; Kajiwara, T.; Funatsu, K.; Terada, K.; Yamabe, M. Polym Eng Sci 1996, 36 2008.
11. Tanoue, S.; Kajiwara, T.; Iemoto, Y.; Funatsu, K. Polym Eng Sci 1998, 38, 409.
12. Tanoue, S.; Iemoto, Y. Polym Eng Sci 1999, 39, 2172.
13. Luo, X. L.; Mitsoulis, E. J Rheol 1989, 33, 1307.
14. Otsuki, Y.; Kajiwara, T.; Funatsu, K. Polym Eng Sci 1997, 37, 1171.
15. Otsuki, Y.; Kajiwara, T.; Funatsu, K. Polym Eng Sci 1999, 39 1969.
16. Laroche, D.; Kabanemi, K. K.; Pecora, L.; DiRaddo, R. W. Polym Eng Sci 1999, 39, 1223.
17. Tanifuji, S. I.; Kikuchi, T.; Takimoto, J. I.; Koyama, K. Polym Eng Sci 2000, 40, 1878.
18. DiRaddo, R. W.; Garcia-Rejon, A. Polym Eng Sci 1993, 33, 653.
19. DiRaddo, R. W.; Garcia-Rejon, A. Adv Polym Technol 1993, 12, 3.
20. Huang, H. X.; Liao, C. M. SPE ANTEC Tech Papers 2002, 48, 804; Polym Test 2002, 21, 745.
21. Huang, H. X.; Liao, C. M. Polym Test 2003, 22, 509.
22. Sarkar, D. ACM Computing Surveys 1995, 27, 519.
23. Dai, H. C.; MacBeth, C. Neural Networks 1997, 10, 1505.
24. Kamarthi, S. V.; Pittner, S. Neural Networks 1999, 12, 1285.
25. Eggen, S.; Sommerfeldt, A. Polym Eng Sci 1996, 36, 336.